DOI: 10.1002/cssc.201100821

Sustainable Production of Syngas from Biomass-Derived Glycerol by Steam Reforming over Highly Stable Ni/SiC

Sung Min Kim and Seong Ihl Woo*[a]

The production of syngas was investigated by steam reforming glycerol over Ni/Al_2O_3, Ni/CeO_2, and Ni/SiC (which have acidic, basic, and neutral properties) at temperatures below 773 K. The complete and stable conversion of glycerol with a yield (higher than 90%) of gaseous products (mainly syngas) was achieved over Ni/SiC during a 60 h reaction, whereas the conversion of glycerol continually decreases over Ni/Al_2O_3 (by 49.8%) and Ni/CeO_2 (by 77.1%). The deactivation of Ni/Al_2O_3 and Ni/CeO_2 is mainly caused by coke deposition because of the C–C cleavage of the byproducts produced by dehydration over acidic sites and condensation over basic sites. Gaseous products with a 1.0–1.9 syngas ratio (H_2/CO) are produced over Ni/SiC. This ratio is required for the Fischer–Tropsch synthesis. However, a syngas ratio of more than 3.0 was observed over Ni/Al_2O_3 and Ni/CeO_2 because of the high activity of the water–gas-shift reaction. Any dissociative or associative adsorption of water on Al_2O_3 and CeO_2 promotes a water–gas-shift reaction and produces a higher syngas ratio. H_2 and CO were mainly produced by decomposition of glycerol through dehydrogenation and decarbonylation over Ni sites. Thus, SiC promotes an intrinsic contribution of nickel (dehydrogenation, and decarbonylation) without any byproducts from the dehydration and condensation.

Introduction

Fossil fuels are the world's main energy source but supplies are diminishing in spite of the growing consumer demand. Environmental issues impact on the use of fossil fuels and have led to the development of clean and sustainable energy. In this era, next-generation biofuels, such as bioalcohol and synthetic biofuels, have become the main substitute for conventional fossil fuels due to technical, economic, and environmental sustainability.[1] Biodiesel, in particular, is a next-generation biofuel and it is considered that it will be important in the future due to its flexibility of manufacture from not only conventional free fatty acids (FFAs) containing animal fats and vegetable oils, but also nonedible oils, such as jatropha and algal oils. Its low sulfur content and potential for reducing global warming is essentially considered as well.[2] The biodiesel market has been expanding (from 7 million tons in 2006 to 18 million tons in 2010). Glycerol is produced as a byproduct of the biodiesel production process and it contains approximately 10 wt% of biodiesel.[3] Although glycerol is used as a raw material in food, pharmaceutical, cosmetic, and tobacco products,[4] the supply of glycerol is greater than the demand because of the increase in biodiesel production. Thus, researchers have been investigating various ways of consuming surplus glycerol.[5]

Of the various types of catalytic conversion of glycerol, this study focused on the production of syngas from steam reforming of glycerol because crude glycerol contains large quantities of water. The process of carbohydrate fermentation and the transesterification of vegetable oil and animal fat produces aqueous glycerol with a weight percentage in the range of 25 to 80 wt%.[4,5d] Thus, steam reforming of glycerol can be conducted without any other pretreatments, such as purification and separation of crude glycerol. The syngas produced by steam reforming of glycerol can be combined with a Fischer–Tropsch (FT) synthesis for the production of fuels and chemicals. The combination of the glycerol steam reforming and the FT synthesis can provide energy-efficient routes for the production of fuels and valuable chemicals. The dual process combines the energy efficiency of the endothermic behavior of glycerol steam reforming and the exothermic behavior of the FT synthesis.[5d] Biosyngas plays a significant role in the production of valuable intermediate feedstocks for the chemical industry because it can be converted into useful biofuels, such as Bio-SNG (synthetic natural gas from biomass), biohydrogen, biomethanol, and FT-fuels.[1]

Metal-supported catalysts such as those based on Pt, Pd, Ni, and Co catalysts have been reported for glycerol steam reforming.[6] Glycerol steam reforming is typically focused on the production of hydrogen over metal-supported catalysts at high temperatures.[6f,h,7] However, the production of syngas by glycerol steam reforming at low temperatures is an energy-efficient route for the production of fuels and chemicals. A nickel-based catalyst is one of the most promising metal-supported cata-

[a] S. M. Kim,[+] Prof. S. I. Woo
Department of Chemical & Biomolecular Engineering
Graduate School of EEWS (WCU)
Korea Advanced Institute of Science and Technology
Daejeon 305-701 (Korea)
Fax: (+82) 42-350-8890
E-mail: siwoo@kaist.ac.kr

[+] Present address:
Clean Energy Research Center
Korea Institute of Science and Technology
Seoul 136-791 (Korea)

lysts because of its low price and high activity for the reforming of glycerol. However, coke deposition is a key problem in steam reforming of glycerol.[6b,g,h,8] Nichio et al. reported that the acidic and basic catalysts, Pt/ZrO_2, Pt/Al_2O_3, and Pt/CeO_2-ZrO_2, promote coke deposition through dehydration- and condensation-induced byproducts, whereas the catalytic activity of the neutral catalyst Pt/SiO_2 for steam reforming of glycerol was maintained for more than 40 h.[6j] In order to improve the catalytic stability, the effect of an additive, such as La_2O_3 and CeO_2, on the Pt/Al_2O_3 catalyst was investigated by Fornasiero et al.,[9] and highly stable catalytic activity for the steam reforming of glycerol was obtained over $Pt/La_2O_3/Al_2O_3$ catalysts. These indicate appropriate supports, and their composition is a prerequisite for obtaining higher activity on steam reforming of glycerol with stability. However, the high syngas ratio (H_2/CO) of Pt/SiO_2 and $Pt/La_2O_3/Al_2O_3$ renders them inapplicable to FT synthesis because of the high activity in the water–gas-shift reaction over oxide supports, which leads to the adsorption of water.[10] Thus, new catalysts should be developed so that syngas can be produced with a suitable ratio,1.0–2.0, for FT synthesis.

Thus, nickel-based catalysts supported on Al_2O_3, CeO_2, and SiC, which typically exhibit acidic, basic, and neutral properties, respectively, were studied for the steam reforming of glycerol in this work. Characterization of the nickel-based catalysts has also been carried out to evaluate the support effect and to compare their activity in the steam reforming of glycerol.

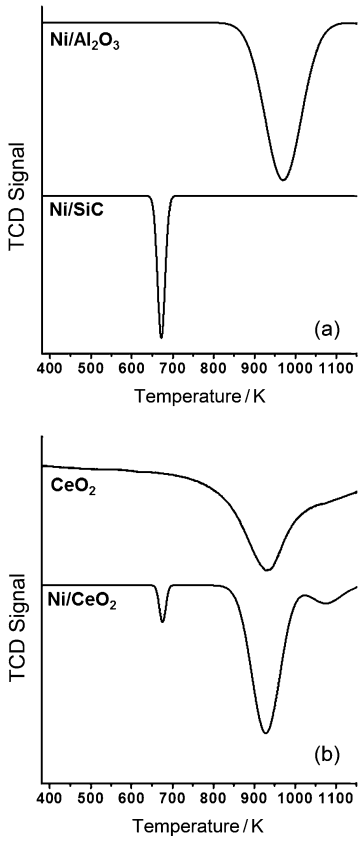

Figure 1. TPR profile of prepared nickel-based catalysts; a) Ni/Al_2O_3 and Ni/SiC, b) CeO_2 and Ni/CeO_2

Results and Discussion

Characterization

The temperature-programmed reduction (TPR) profiles of prepared nickel-based catalysts are described in Figure 1. In the case of CeO_2, the reduction of surface Ce^{4+} into Ce^{3+} was caused by hydrogen spillover where the reduction occurred at the interface of the metal (Ni in this study) and CeO_2.[11] This phenomenon could be supported by TPR results. As reported by Kunkes et al. for $Pd/CeZrO_x$,[12] the low-temperature reduction peak at 480 K was assigned to the reduction of Pd and of ceria species in intimate contact with the metal, whereas the broad peak centered at 720 K was assigned to the reduction of surface ceria species that are not in contact with the metal. The latter reduction was shifted to lower temperature from 860 K on $CeZrO_x$ due to hydrogen spillover from the metal. This could also be caused by the high value of metal dispersion measured for the CeO_2 based catalysts. Thus, we conducted TPR experiments for both Ni/CeO_2 and CeO_2. As shown in Figure 1 (b), CeO_2 shows a high-temperature reduction peak centered at about 928 K, which is almost identical to the peak for Ni/CeO_2 with the reduction of Ni at 673 K. This finding suggests that the hydrogen spillover from Ni to surface ceria species is negligible for the Ni/CeO_2 prepared in this work. Thus, we did not strongly consider the occurrence of hydrogen spillover on Ni/CeO_2. Nevertheless, the metal dispersion of Ni/CeO_2 appears to be relatively high. In order to estimate the CO spillover on Ni/CeO_2, the Ni particle size was measured by chemisorption, XRD, and scanning transmission electron microscopy (STEM). Identical Ni particle sizes were observed. This indicates that spillover of hydrogen from Ni to surface ceria species, and overestimation of metal dispersion are restricted in this work.

The results of physical and chemical analyses for the prepared nickel-based catalysts are summarized in Table 1. The catalyst with the highest specific surface area and metal dispersion was Ni/Al_2O_3, followed by Ni/CeO_2, and Ni/SiC. The

Table 1. Physical and chemical analyses of the nickel-based catalysts.

Catalyst	SA[a] [$m^2 g_{cat}^{-1}$]	d[b] [%]	CO uptake [$\mu mol\, g_{cat}^{-1}$]	PS_{chemi}[c] [nm]	PS_{XRD}[d] [nm]	PS_{STEM}[e] [nm]	NH_3-TPD[f] [$\mu mol\, g_{cat}^{-1}$]	CO_2-TPD[f] [$\mu mol\, g_{cat}^{-1}$]
Ni/Al_2O_3	54.3	10.5	127.8	9.6	9.7	9.2	412	68
Ni/CeO_2	41.7	5.3	64.4	19.1	20.1	18.9	0	352
Ni/SiC	32.2	2.8	34.1	36.5	35.9	33.9	0	32

[a] Specific surface areas were determined by BET analysis. [b] Metal dispersion measured by chemisorption. [c] Average particle size of nickel obtained from chemisorption (with the assumption of a spherical geometry). [d] Average particle size of the nickel crystal as determined by Scherrer's equation. [e] Average nickel particle size measured by STEM. [f] Total desorbed amount of NH_3 or CO_2.

order of metal dispersion corresponds with the specific surface area, indicating that a high surface area induces high nickel dispersion. Although Ni/Al_2O_3 was reduced at a higher temperature than Ni/CeO_2 and Ni/SiC, it showed the highest metal dispersion among the prepared nickel-based catalysts. The prepared nickel-based catalyst with the lowest nickel dispersion and specific surface area was Ni/SiC.

The XRD patterns of the reduced nickel-based catalysts at each temperature determined by TPR are shown in Figure 2. All the nickel-based catalysts show metallic nickel peaks. In the case of Ni/SiC, which was calcined at 873 K in air, the peaks indicate nickel and SiC but no oxide species such as SiO_2. This result suggests that SiC is not easily oxidized and maintains its carbide state under oxidizing conditions. Moreover, the peaks representing Ni and Al_2O_3 were mainly observed in the XRD profile of Ni/Al_2O_3. A slight shift in the peaks from $2\theta = 67^\circ$ for γ-Al_2O_3 to $2\theta = 66^\circ$ representing the diffraction peak for the (440) plane of $NiAl_2O_4$ was also observed. This indicates that metallic Ni, Al_2O_3, and $Ni_2Al_2O_4$ coexist in reduced Ni/Al_2O_3 catalysts. This is in accordance with the work of Li et al.[13]

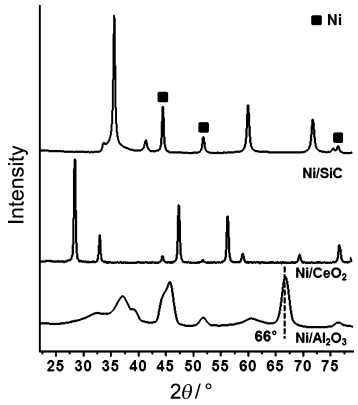

Figure 2. X-ray diffraction profile of reduced nickel-based catalysts

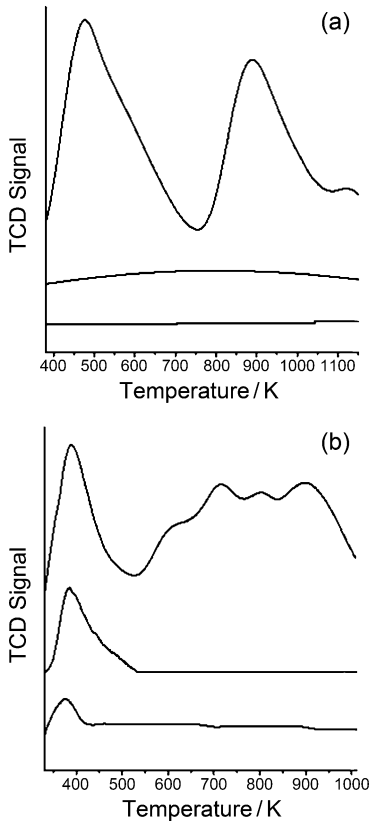

Figure 3. a) NH_3-TPD and b) CO_2-TPD profiles of the reduced nickel-based catalysts.

The profile of NH_3 and CO_2 temperature-programmed desorption (TPD) is shown in Figure 3, and the total amount of desorbed NH_3 and CO_2 is summarized in Table 1. Peaks of NH_3 desorption at 475 and 880 K can be observed over Ni/Al_2O_3, but there are no peaks over Ni/CeO_2 and Ni/SiC. The amount of NH_3 desorbed from Ni/Al_2O_3 was 228 $\mu mol\,g^{-1}$ at 475 K and 182 $\mu mol\,g^{-1}$ at 880 K (Figure 3a). In the case of the CO_2-TPD (Figure 3b), there are many peaks over Ni/CeO_2 in the temperature range investigated, but only a single peak at 370 K over Ni/Al_2O_3 and Ni/SiC. In the case of Ni/Al_2O_3 and Ni/SiC, the CO_2 was mainly physically adsorbed.[14] The amount of CO_2 desorbed from Ni/CeO_2 was 82 $\mu mol\,g_{cat}^{-1}$ for temperatures below 500 K and 270 $\mu mol\,g_{cat}^{-1}$ for temperatures above 500 K. Amounts of 68 and 32 $\mu mol\,g_{cat}^{-1}$ of physically adsorbed CO_2 were measured over Ni/Al_2O_3 and Ni/SiC, respectively. These results indicate that Ni/SiC has no functionality, whereas Ni/Al_2O_3 and Ni/CeO_2 clearly have acidic and basic properties, respectively.

Figure 4 shows STEM images of the reduced catalysts. In the case of Ni/Al_2O_3, the nickel particle size is smaller than 10 nm and the nickel particles are well dispersed on the Al_2O_3. In contrast, the nickel particles tend to agglomerate and form particles larger than 20 nm on CeO_2. In the case of Ni/SiC, which has the largest nickel particles, the particles have a distributed size of around 40 nm on the SiC. The nickel particles are well dispersed on the SiC surface. These results imply that the interaction of nickel and SiC is much weaker than that of the other prepared nickel-based catalysts. During the calcination, reduction, and reaction processes, nickel particles on SiC become larger than those on Ni/Al_2O_3 and Ni/CeO_2.

Effect of support on production of syngas and hydrogen

The activity of glycerol reforming can be affected by the support properties. To investigate the effect of the support on the production of syngas and hydrogen, the reaction parameters were varied for the conversion of aqueous glycerol by steam reforming. First, the reaction was conducted in a temperature range of 573–773 K. Table 2 shows that the complete conversion of glycerol occurred over Ni/Al_2O_3 and Ni/CeO_2 at temperatures higher than 673 K and over Ni/SiC at 773 K.

This result is due to the fact that the nickel particles on Al_2O_3 and CeO_2 are smaller and more highly dispersed than those on SiC. At temperatures above 623 K, Ni/Al_2O_3 and Ni/CeO_2 have a H_2/CO ratio higher than 2.3 and a CO/CO_2 ratio lower than 2.4. This result indicates that the water–gas-shift reaction vigorously produces hydrogen over Ni/Al_2O_3 and Ni/

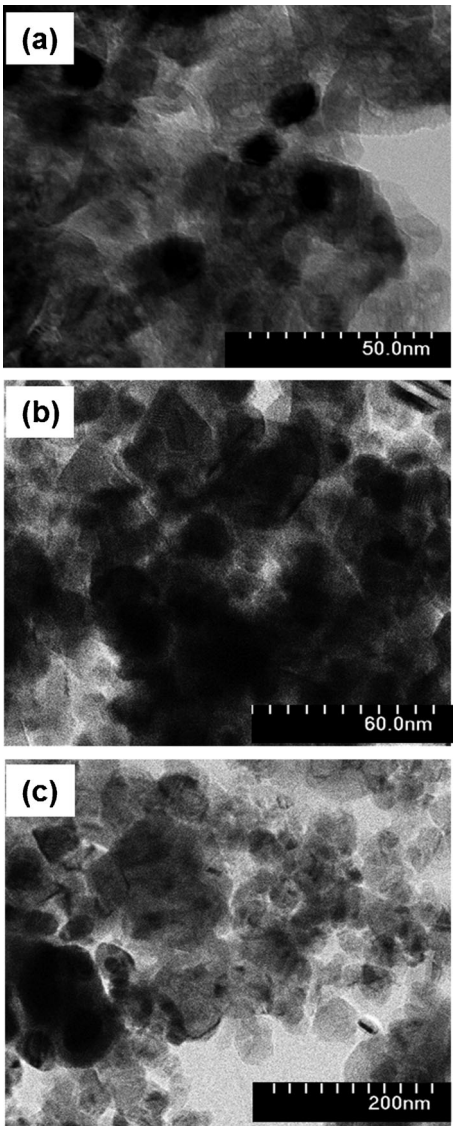

Figure 4. STEM images of reduced nickel-based catalysts: a) Ni/Al_2O_3, b) Ni/CeO_2, and c) Ni/SiC.

Table 2. Effect of reaction temperature on the molar ratio of the main gaseous products during the glycerol steam reforming experiments.[a]

Catalyst	T[b] [K]	Conv.[c] [%]	Molar ratio H_2/CO	CO/CO_2	CH_4/H_2	X_{gas}[d] [%]
Ni/Al_2O_3	573	82.0	1.3	5.3	0.14	20.1
	623	97.0	2.3	2.4	0.11	56.4
	673	100	4.4	0.5	0.11	62.2
	773	100	4.9	0.4	0.09	92.7
Ni/CeO_2	573	72.2	1.0	4.7	0.2	20.3
	623	96.4	2.5	2.3	0.05	42.4
	673	98.7	3.0	1.2	0.05	59.7
	773	100	4.8	0.5	0.05	87.3
Ni/SiC	573	56.6	1.0	–	0.30	15.9
	623	74.4	1.2	45.2	0.07	67.9
	673	91.8	1.3	27.4	0.06	74.6
	773	100	1.7	3.0	0.05	93.7

[a] Reaction conditions: WGMR of 6:1, FFR of 0.15 mL min^{-1} (LHSV = 33.3 h^{-1}), and atmospheric pressure. [b] Reaction temperature. [c] Conversion of glycerol (%) = (inlet of glycerol − outlet of glycerol)/inlet of glycerol × 100. [d] Conversion of glycerol into a gaseous phase (%) = $(R_{i-outlet} \times N)_{gas}/(R_{Glycerol-inlet} \times N_{Glycerol}) \times 100$, where R and N represent the molar flow rate and the carbon number, respectively, of CO, CO_2, and CH_4.

CeO_2. The water–gas-shift reaction is known to be active over catalysts supported on acidic and basic oxides such as CeO_2 and Al_2O_3.[15] This level of activity occurs because these oxide supports offer dissociative and associative sites for the adsorption of water and the metal provides a site for the adsorption of CO. Formate is generated between the adsorbed water and CO and then decomposes into H_2 and CO_2 as a result of dehydration over the acidic oxide support and dehydrogenation over the basic oxide support. However, the nonoxide-supported catalyst Ni/SiC has a lower syngas ratio (1.0–1.7) and a higher CO/CO_2 ratio (3.0–45.2) than Ni/Al_2O_3 and Ni/CeO_2. The much higher CO/CO_2 ratio (above 40) was caused by the low catalytic activity of the water–gas-shift reaction. The syngas produced over Ni/SiC has a syngas ratio of about 1.5; this value, which is in agreement with our expected value, suggests that the syngas can be used for FT synthesis. It confirms that the water–gas-shift reaction is active on the oxide-supported catalysts Al_2O_3 and CeO_2 but not on SiC. The activity of the glycerol steam reforming and the water–gas-shift reaction is lower over Ni/SiC than over Ni/Al_2O_3 and Ni/CeO_2. However, the conversion of glycerol into a gaseous-phase product containing CH_4, CO, and CO_2 tends to occur at a higher rate over Ni/SiC than over Ni/Al_2O_3 and Ni/CeO_2. These results imply that the Ni/SiC catalyst is more suitable for the production of syngas than the oxide-supported catalysts Ni/Al_2O_3 and Ni/CeO_2.

To further demonstrate the effect of oxides and nonoxides on the production of syngas and hydrogen, the water to glycerol molar ratio (WGMR) was varied for glycerol steam reforming over the prepared nickel-based catalysts at 673 K. The molar ratio of water to glycerol was varied from 3:1 (63 wt% of glycerol) to 9:1 (36 wt% of glycerol) because 25–80 wt% of aqueous crude glycerol is produced during the transesterification process in the production of biodiesel.[4,5d] The results are presented in Table 3. The conversion of glycerol into gaseous products increases as the WGMR increases because the concentration of glycerol is diluted when the WGMR is increased. The H_2/CO and CO/CO_2 ratio over the oxide-supported catalysts Ni/Al_2O_3 and Ni/CeO_2 is significantly affected by the WGMR because of the water–gas-shift reaction. The increase of water content in the feed promotes a forward reaction of the water–gas-shift reaction, which produce hydrogen and carbon dioxide from water and carbon monoxide. Thus, the H_2/CO ratio increased to 12.7 and the CO/CO_2 ratio decreased to 0.2 as the WGMR increased to 9:1 over the oxide-supported catalysts, especially Ni/Al_2O_3. The influence of the water content was also exhibited over Ni/SiC. However, because of the inactivity of Ni/SiC

Table 3. Effect of the molar ratio of water to glycerol on the molar ratio of the main gaseous products during the glycerol steam reformation experiments.[a]

Catalyst	WGMR[b]	Conv. [%]	Molar ratio H_2/CO	CO/CO_2	CH_4/H_2	X_{gas} [%]
	3:1	96.8	2.7	1.1	0.10	46.4
Ni/Al_2O_3	6:1	100	4.4	0.5	0.11	62.2
	9:1	100	12.7	0.2	0.06	73.0
	3:1	90.8	2.5	1.7	0.13	50.5
Ni/CeO_2	6:1	98.7	3.0	1.2	0.05	59.7
	9:1	100	6.4	0.4	0.04	87.7
	3:1	83.0	1.3	117.8	0.07	65.7
Ni/SiC	6:1	91.8	1.5	27.4	0.06	74.6
	9:1	100	1.8	14.1	0.06	95.2

[a] Reaction conditions: A reaction temperature of 673 K, FFR of 0.15 mL min^{-1} (LHSV = 33.3 h^{-1}), and atmospheric pressure. [b] Water to glycerol molar ratio.

in the water–gas-shift reaction, we observed no significant change of H_2/CO over Ni/SiC, only a slight increase of the H_2/CO ratio, and a decrease of CO/CO_2. This result confirms that catalysts supported on acidic and basic oxide are unsuitable for producing syngas because of their higher hydrogen yield and lower CO yield.

ratio (H_2/CO) was lower than 2.2, which is much lower than those for Ni/Al_2O_3 (12.8) and Ni/CeO_2 (6.4) under the same conditions, although they contained similar Ni particle sizes. This is because the activity in the water–gas-shift reaction is significantly governed by the catalytic properties of the support, although the addition of Ni promotes the activity. In other words, the water–gas-shift reaction is inactive over SiC, and Ni/SiC is appropriate for the production of syngas for FT synthesis by the steam reforming of glycerol.

The catalytic stability of prepared 1.0–10.0 wt% Ni/SiC catalysts was also tested (Figure 5). The catalytic activity in the steam reforming of glycerol and the H_2/CO molar ratio were maintained for 20 h. This confirmed the correlation between metal loading and H_2/CO ratio. These findings suggest that the sustainable production of syngas from the steam reforming of glycerol can be accomplished over Ni/SiC.

Effect of Ni particle size over Ni/SiC

To elucidate the effect of the properties of the support, the steam reforming of glycerol was carried out over 1.0–10.0 wt% Ni/SiC, where the reaction temperature, pressure, feed flow rate (FFR), and WGMR were 673 K, atmospheric pressure, 0.15 mL min^{-1} [liquid hourly space velocity (LHSV) of 33.3 h^{-1}], and 9:1, respectively. The CO uptake, metal dispersion, and Ni particle size were calculated by CO chemisorptions and are summarized in Table 4.

Table 4. Effect of the Ni loading on the molar ratio of the main gaseous products during the glycerol steam reformation experiments over Ni/SiC.[a]

Nominal Ni [wt%]	d[b] [%]	CO uptake [μmol g_{cat}^{-1}]	PS_{chemi}[c] [nm]	Conv. [%]	Molar ratio H_2/CO	CO/CO_2	CH_4/H_2	X_{gas} [%]
1.0	11.0	13.4	9.2	50.7	2.2	5.2	0.05	40.4
3.0	7.0	25.6	14.4	63.4	2.0	9.1	0.05	48.1
5.0	4.4	27.0	22.8	74.1	1.9	11.2	0.05	70.2
7.0	3.5	29.5	29.2	89.1	1.8	13.5	0.06	82.3
10.0	2.8	34.1	36.5	100	1.8	14.1	0.06	95.2

[a] Reaction conditions: A reaction temperature of 673 K, WGMR of 9:1, FFR of 0.15 mL min^{-1} (LHSV of 33.3 h^{-1}), and atmospheric pressure. [b] Metal dispersion measured by chemisorption. [c] Average particle size of nickel obtained from chemisorption (with the assumption of a spherical geometry).

As the Ni loading on SiC decreased, the metal dispersion increased from 2.8% to 11.0%, whereas Ni particle size and the amount of CO uptake decreased (from 36.5 to 13.4 nm for the former and from 34.1 to 13.4 μmol g_{cat}^{-1} for the latter). As a result, the conversion of glycerol decreased from 100 to 50.7%. This indicates that the catalytic conversion of glycerol by steam reforming is affected by the absolute amount of Ni sites. On the other hand, the H_2/CO ratio increased and the CO/CO_2 ratio decreased as the Ni particle size became smaller. This indicates that the activity of the water–gas-shift reaction is enhanced by smaller Ni particles. This corresponds well with the fact that Ni addition in small amounts enhanced the catalytic activity of the water–gas-shift reaction, whereas higher metal contents led to bulk particle formation and a negligible contribution to the catalytic activity.[15b] However, the syngas

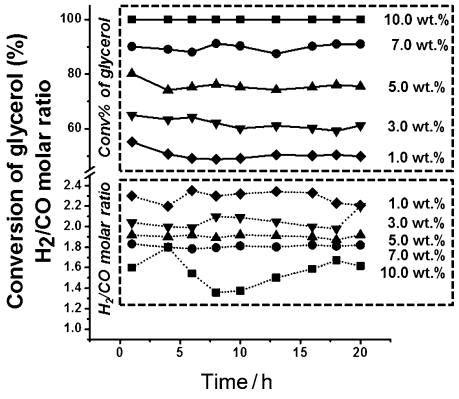

Figure 5. Stability tests of 1.0–10.0 wt% Ni/SiC at a temperature of 673 K, a WGMR of 9:1, a FFR of 0.15 mL min^{-1} (LHSV of 33.3 h^{-1}), and atmospheric pressure.

Effect of contact time over Ni/SiC

The above results confirmed that Ni/SiC is suitable for producing syngas. Thus, we focused on understanding the catalytic behavior of Ni/SiC. The conversion of glycerol into gaseous products, especially syngas, is greater over Ni/SiC than over Ni/Al_2O_3 and Ni/CeO_2. The difference in activity for the production of syngas came from the competitive activity between dehydrogenation (for the production of hydrogen) and decarbonylation (for the production of carbon monoxide) over nickel sites and side reactions, such as dehydration and condensation over the acidic sites of Al_2O_3 and the basic sites of CeO_2. That is, the nickel sites over neutral SiC have only an intrinsic contribution without side reactions at acidic or basic sites. Thus, the use of Ni/SiC resulted in higher yields of syngas.

To confirm and further study the catalytic behavior over Ni/SiC, steam reforming was conducted by varying the FFR from 0.08 (LHSV = 17.8 h^{-1}) to 0.5 mL min^{-1} (LHSV = 111 h^{-1}). Table 5 shows that the glycerol was completely converted and that 95% of it was converted into gaseous products. Furthermore, there was a syngas ratio of 1.8–1.9 for an FFR value of less than 0.15 mL min^{-1} (LHSV = 33.3 h^{-1}). However, the activity of the glycerol reforming was drastically decreased when the FFR exceeded 0.3 mL min^{-1} (LHSV = 66.6 h^{-1}). When the FFR increased to 0.5 mL min^{-1} (LHSV = 111 h^{-1}), the H_2/CO ratio dropped to 1.2, the CO/CO_2 ratio increased to 53.3 and the CH_4/H_2 ratio increased to 0.22. These results indicate that sufficient contact time is required for the production of hydrogen and carbon monoxide by dehydrogenation and decarbonylation. The portion of liquid products produced over Ni/SiC at an FFR of more than 0.3 mL min^{-1} exceeds 40%. Thus, an analysis of the liquid products can help identify the reaction mechanism of the glycerol reforming.

Table 6. Product distribution from the conversion of glycerol steam reformation over the catalyst Ni/SiC at 673 K.[a]

Catalyst	FFR [mL min^{-1}]	X_{liq} [%]	Carbon selectivity[b] methanol	acetic acid	acetol	ethylene glycol	1,3-dihydroxy-2-propanone	acetone
Ni/SiC	0.08	0	0	0	0	0	0	0
	0.15	4.8	0.48	0.02	0.08	0.13	0.20	0.09
	0.3	33.6	0.27	0.01	0.11	0.10	0.44	0.1
	0.5	45.7	0.07	0	0.17	0.09	0.53	0.14

[a] Reaction conditions: reaction temperature of 673 K, WGMR of 9:1, and atmospheric pressure. [b] The carbon selectivity of liquid phase products = $(R_{i-outlet} \times N)_{liq} / \Sigma (R_{i-outlet} \times N)_{liq} \times 100$, where R and N represent the molar flow rate and the carbon number of given species (i), respectively.

Table 5. Effect of the FFR on the molar ratio of the main gaseous products during the glycerol steam reformation experiments over Ni/SiC.[a]

FFR[b] [mL min^{-1}]	LHSV [h^{-1}]	Conv. [%]	Molar ratio H_2/CO	CO/CO_2	CH_4/H_2	X_{gas} [%]
0.08	17.8	100	1.9	10.6	0.07	100
0.15	33.3	100	1.8	14.1	0.06	95.2
0.3	66.6	68.1	1.3	33.8	0.10	66.4
0.5	111	42.8	1.2	53.3	0.22	53.4

[a] Reaction conditions: reaction temperature of 673 K, WGMR of 9:1, and atmospheric pressure. [b] The FFR of aqueous glycerol.

Proposed reaction pathway of glycerol steam reforming

To study the reaction mechanism of glycerol steam reforming, gas chromatography–mass spectrometry (GC–MS) was carried out for qualitative analysis of the liquid produced over the prepared nickel-based catalysts. Table 6 shows that the liquid-phase products increased as the FFR of the aqueous glycerol solution increased. Significant amounts of methanol and 1,3-dihydroxy-2-propanone and slight amounts of acetic acid, 1-hydroxy-2-propanone (acetol), ethylene glycol, and 2-propanone (acetone) were produced over Ni/SiC during the reaction. The amounts of these liquid products as well as the following: 2-methyl-cyclopentanone, ethylene glycol, propylene glycol, butanal, and 5-hydroxy-2-methyl-1,3-dioxane were mainly produced over Ni/Al_2O_3 and Ni/CeO_2. The reaction pathway of glycerol steam reforming over nickel-based catalysts was suggested based on these quantitative and qualitative analyses by means of GC–MS and gas chromatography with a flame ionization detector (GC–FID, Figure 6).

First, the glycerol undergoes not only dehydration into acetol and 3-hydroxypropanal, but also dehydrogenation into 1,2-dihydroxypropanal over acid/base sites and metal sites, respectively. The Ni/SiC catalyst promotes the intrinsic metal activity without any support-induced side reactions. Thus, ethylene glycol is produced by the subsequent decarbonylation of 1,2-dihydroxypropanal. 2-Hydroxyacetaldehyde and formaldehyde were also produced from 1,2-hydroxypropanal by retroaldol condensation. In addition, the continuous dehydrogenation and decarbonylation produces methanol, hydrogen, and carbon monoxide. In the case of Ni/Al_2O_3 and Ni/CeO_2, the metal contribution (the dehydrogenation and decarbonylation) competes with the support contribution (the dehydration and condensation). Acrolein (propenal) can be produced by the dehydration of 1-hydroxypropanal obtained by the dehydration of glycerol, however, it requires high acidity.[16] Thus, the production of acrolein was restricted over the prepared catalysts. 1-Hydroxypropanal also subsequently underwent decarbonylation and resulted in the production of ethanol. Ethanol was then converted into syngas and methane. Acetol is produced by the hydrogenation of 1,3-dihydroxy-2-propanone and/or the dehydration of glycerol. 2-Methylcyclopentanone was subsequently produced by the continuous condensation and hy-

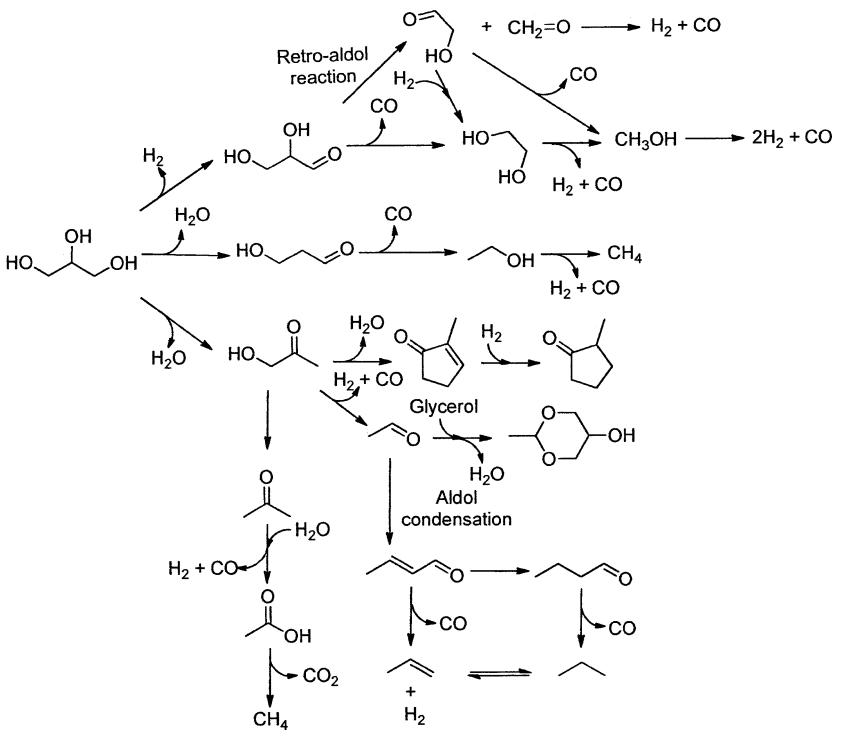

Figure 6. Proposed reaction pathway of glycerol steam reforming over nickel-based catalysts.

drogenation of acetol over acid/base sites. The hydrogenation of acetol produces acetone, and simultaneously the dehydrogenation with decarbonylation of acetol produces acetaldehyde. The intercondensation between acetaldehyde and glycerol produces 5-hydroxy-2-methyl-1,3-dioxane, and the self-condensation (aldol condensation) of acetaldehyde with hydrogenation produces butanal.[17] Propane and CO were then produced by the decarbonylation of butanal. Acetic acid was produced not only by the steam reforming of acetone, but also the oxidation of acetaldehyde. As a result of the decarbonylation of acetic acid, methane was obtained. This mechanistic study of glycerol steam reforming over nickel-based catalysts suggests that intrinsic metal activity helps achieve a higher yield of syngas by promoting dehydrogenation and decarbonylation. On the other hand, acid/base sites promoted the reaction of not only dehydration, but also condensation, such as aldol condensation. These findings suggest that promoting the Ni contribution was a mandatory requirement for the production of syngas, whereas valuable chemicals, such as ethylene glycol and alcohols, were obtained over acid/base sites. Thus, control of the contributions between metal and acid/base sites plays a significant role for the production of biofuels.

Stability test and study of deactivation

To compare the durability of the studied catalysts, steam reforming of glycerol was carried out over the prepared nickel-based catalysts for 60 h, where WGMR, FFR and temperature were 9:1, 0.15 mL min^{-1} (LHSV = 33.3 h^{-1}), and 673 K, respectively. The conversion of glycerol on the studied nickel-based catalysts was completed in 20 h. On the Ni/Al_2O_3 and Ni/CeO_2 catalysts, the glycerol conversion gradually decreased, but on Ni/SiC, the conversion of glycerol remained at 100%. By the end of the reaction, 49.8% of the glycerol on Ni/Al_2O_3 and 77.1% of the glycerol on the Ni/CeO_2 had been converted (Figure 7a).

As shown in Figure 7b, the conversion of glycerol to gaseous products was in the range of 59.6 to 31.5% for the glycerol on Ni/Al_2O_3. This value is slightly less than the corresponding range of 84.3 to 53.7% for glycerol on Ni/CeO_2. When the oxide-supported catalysts Ni/

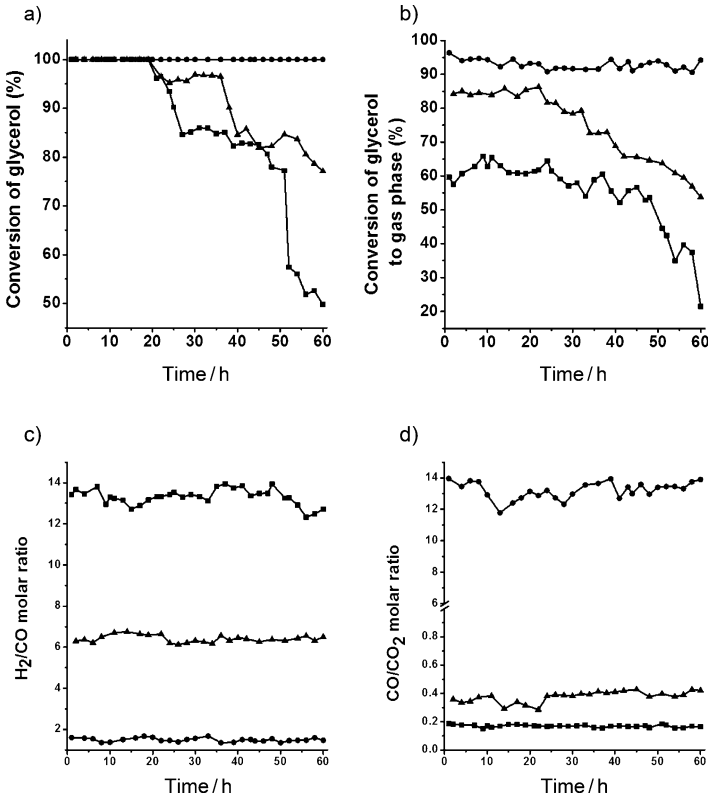

Figure 7. Stability tests of nickel-based catalysts at a temperature of 673 K, a WGMR of 9:1, an FFR of 0.15 mL min^{-1}, and atmospheric pressure; the time-on-stream of a) the conversion of glycerol, b) the conversion of glycerol into gas-phase products, c) the H_2/CO molar ratio, and d) the CO/CO_2 molar ratio for nickel supported on Al_2O_3 (■), CeO_2 (▲), and SiC (●).

Al_2O_3 and Ni/CeO_2 are used, the syngas ratio is higher than 6 and the CO/CO_2 ratio is lower than 0.4 (Figures 7c and d). As mentioned above, a high syngas ratio is inappropriate for an FT synthesis. However, when Ni/SiC is used, the syngas ratio is between 1.5 and 1.7, glycerol is completely converted, and more than 90% of the glycerol is converted into gaseous products. This result indicates that Ni/SiC has the highest stability of all the studied nickel-based catalysts with regard to the production of syngas; furthermore, there is a significant deactivation over Ni/Al_2O_3 and Ni/CeO_2.

After the stability test, the Ni-based catalysts were collected and characterized for the purpose of investigating the deactivation process. Nickel-based catalysts are known for their high reforming activity.[6b,h,18] However, coke deposition and methane formation are disadvantages of nickel-based catalysts.[8,19] To investigate the coke deposition on the used nickel-based catalysts, temperature-programmed oxidation (TPO), thermogravimetric/differential thermal analysis (TG/DTA), and STEM analyses were conducted. As a result of the oxidation of the used catalysts under 20% of O_2/He, the deposited coke was oxidized into carbon dioxide (Figure 8a). In the case of the catalysts that underwent deactivation, the TG/DTA in air reveals that the weight loss was 59.84% for Ni/Al_2O_3 and 9.47% for Ni/CeO_2 but only 2.7% for Ni/SiC (Figures 8b and c). This result implies that a significant amount of coke was deposited on Ni/Al_2O_3 and Ni/CeO_2 and that the catalytic activity was mainly deactivated by the coke deposition. Coke deposition on nickel-based catalysts is generally attributed to the high C–C cleavage activity of nickel. A significant amount of coke was deposited as a result of the C–C cleavage of dehydration-induced intermediates (such as oxygenated and olefin species).[5d,8,19,20] the coke deposition during the reaction is mainly due to the C–C cleavage of byproducts produced by dehydration and condensation. In particular, the TPO and DTA peaks of Ni/CeO_2 occurred at 590 K, which is a much lower temperature than that of the peaks of Ni/Al_2O_3 and Ni/SiC (Figures 8a and c). CeO_2 is known to have a high oxygen storage capacity and a high resistance to coke deposition.[7a,21] The oxygen in CeO_2 reacts with the surface coke, producing a soft coke deposition, which can be removed at a low temperature.

The coke deposition of the used catalysts was confirmed by the STEM mapping analysis. As shown in Figure 9, the coke entirely covers the surface of Ni/Al_2O_3 and Ni/CeO_2 but not Ni/SiC. In particular, there is a carbon whisker in the STEM image of the nickel-based catalysts. The formation of carbon whiskers in the steam reforming process is a well-known fact.[20] The carbon encapsulates the surface nickel, an active site, and then it forms nickel carbide. The nickel carbide is not stable under steam reforming conditions. Thus, the carbon nucleates form filaments, which grow into carbon filaments during the reaction. The results indicate that coke deposition is critical for glycerol steam reforming over a nickel-based catalyst. Resistance to coke deposition is therefore a prerequisite for glycerol steam reforming over nickel-based catalysts. Higher coke resistance was accomplished over Ni/SiC, and as a result pronounced stability was obtained. This characteristic property is in accordance with the dry reforming of methane over Ni/SiC:

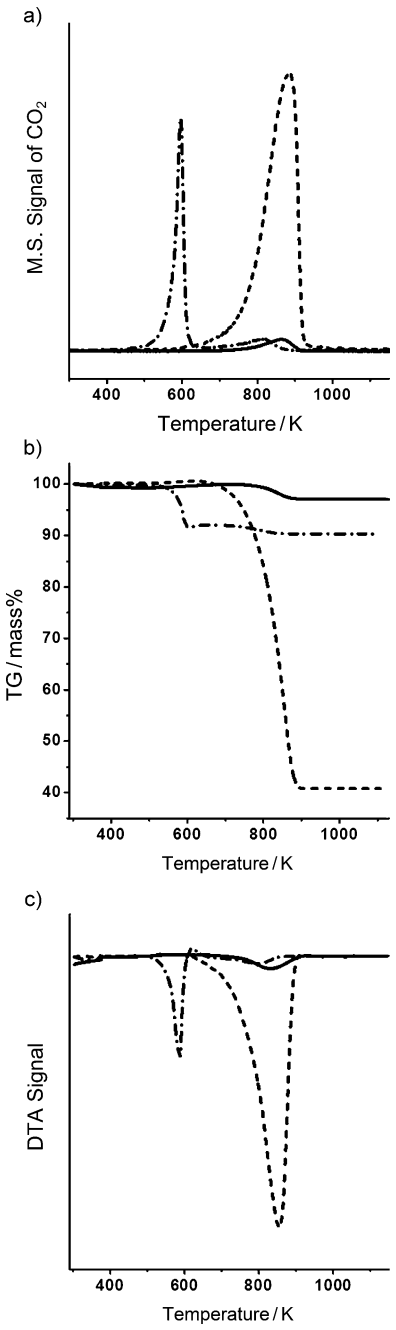

Figure 8. Deactivation test of nickel-based catalysts reacted for 60 h at a temperature of 673 K, a WGMR of 9:1, an FFR of 0.15 mL min^{-1}, and at atmospheric pressure; a) TPO, b) TG, and c) DTA for nickel supported on Al_2O_3 (dash), CeO_2 (dash–dot), and SiC (solid line).

higher coke resistance and stability were achieved over Ni/SiC.[22] From this point of view, Ni/SiC is a promising catalyst for the production of syngas by glycerol steam reforming as shown by the pronounced coke resistance.

Conclusions

The production of syngas by the steam reforming of glycerol over Ni/SiC leads to a high yield of syngas, and the catalyst has outstanding stability. The neutral properties of SiC pro-

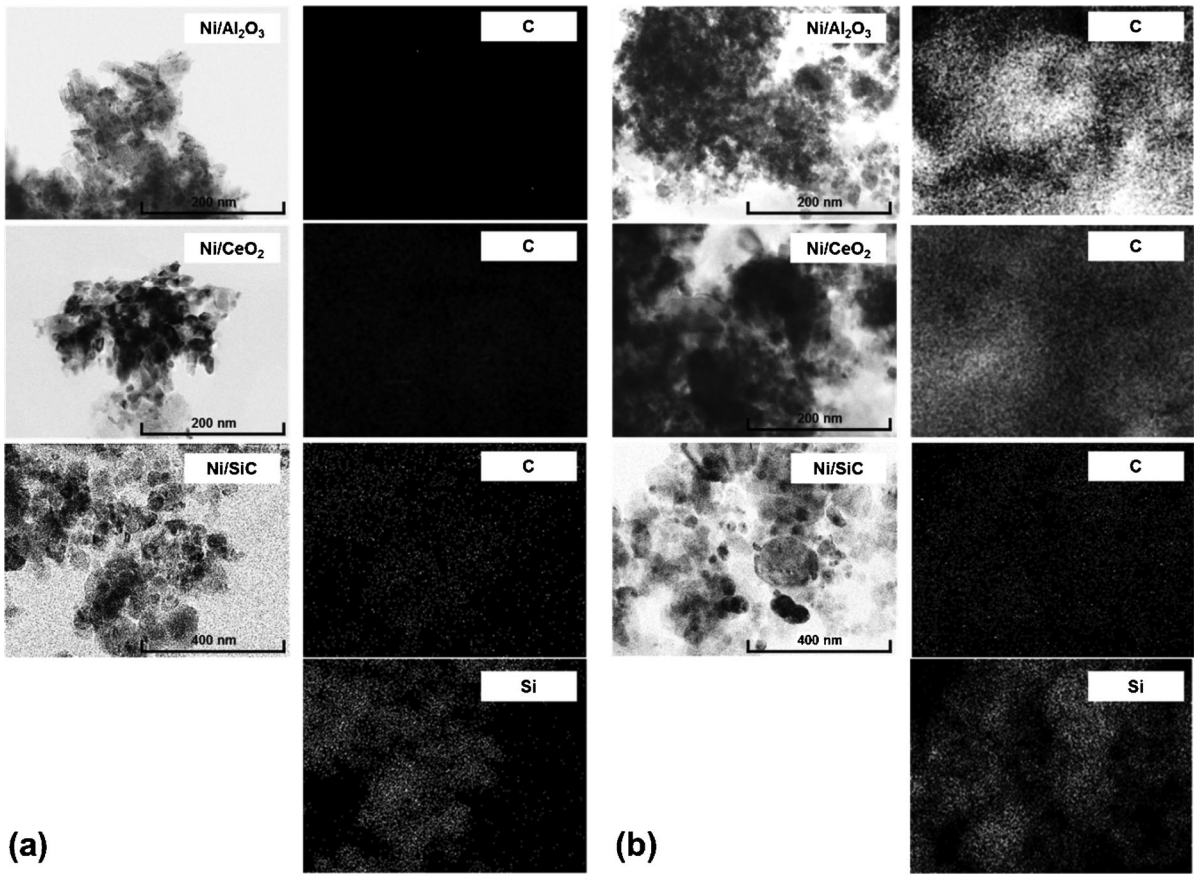

Figure 9. STEM and mapping image of nickel-based catalysts: a) reduced catalysts, b) catalysts after 60 h of reaction at a temperature of 400 °C, a WGMR of 9:1, an FFR of 0.15 mL min^{-1}, and atmospheric pressure.

mote an intrinsic nickel contribution to glycerol steam reforming, especially in terms of dehydrogenation and decarbonylation. At the same time, there are minimal side reactions from the condensation induced by the basic properties and the dehydration induced by the acidic properties. This feature of Ni/SiC contributes to the high stability of glycerol steam reforming and the low level of coke deposition. An appropriate syngas ratio for the FT synthesis can be achieved over Ni/SiC because the nonoxide support SiC is more inactive in a water–gas-shift reaction than the oxide supports Al_2O_3 and CeO_2.

In conclusion, nickel-based catalysts promote the production of syngas by glycerol steam reforming. This effect is due to the intrinsic nickel contribution, particularly the dehydrogenation and decarbonylation, over Ni/SiC. The process minimizes the coke deposition and side reactions.

Experimental Section

Catalyst preparation: Nickel-based catalysts were prepared over γ-Al_2O_3 (Alfa Aesar), CeO_2, and SiC (Sigma–Aldrich). The catalysts were prepared by using a traditional impregnation method with $Ni(NO_3)_2{\cdot}6H_2O$ (Sigma–Aldrich). A nominal 1–10 wt% Ni was loaded onto all the supports. The prepared catalysts were dried at 383 K overnight and calcined at 873 K for 2 h in air. The calcined catalysts were ground and sieved under 200 μm.

Catalytic activity test: The glycerol steam reforming was conducted in a quartz reactor (length: 15 in; diameter of the inlet: 1/4 in; diameter of the bed: 1 in), where 0.5 g of calcined catalyst was packed in the middle. Prior to the activity test, the catalyst was reduced over 1 h by TPR at a given temperature with 20 vol% of H_2/Ar. The reaction system was equilibrated for 1 h at a certain temperature in the range of 573 to 773 K in a stream of Ar. An aqueous glycerol solution with a certain molar ratio of glycerol and water was fed by a liquid pump into the heating zone and gasified at 523 K. The gasified reactant was introduced into the catalyst bed with Ar at a rate of 20 mL min^{-1}. The liquid-phase products, unreacted glycerol, and water were condensed and collected in a separator, which was kept at 278 K; they were then analyzed with a GC equipped with a flame ionization detector and a DB-WAX column. A GC equipped with a thermal conductivity detector was also used to analyze the gaseous products. A molecular sieve 5A was used for the analysis of H_2, CO, and CH_4, and porapak Q was used for the analysis of CO_2.

Characterization of catalysts: 1) TPR and TPO were conducted with a mass spectrometer (Hiden Analytical Ltd.). Prior to the TPO and TPR, we dehydrated and degassed the catalysts at 373 K for 2 h under He. Our analysis was conducted at 373–1173 K with a heating rate of 5 K min^{-1} with less than 5 vol% H_2/Ar (30 mL min^{-1}) and with less than 10 vol% O_2/He (50 mL min^{-1}) for the TPR and TPO, respectively. We used a mass spectrometer to trace H_2 and H_2O for the TPR and CO, CO_2, H_2O, and O_2 for the TPO. 2) TPD experiments with CO_2 and NH_3 were conducted by using a BEL-CAT instrument (BEL Japan, Inc.) equipped with a ther-

mal conductivity detector (TCD). For 1 h, the prepared catalysts were loaded and reduced in H_2 for each temperature determined by the TPR. The reactor was then purged with He at 623 K for 30 min and cooled to 313 K for CO_2 adsorption or 473 K for NH_3 adsorption. After the reduced catalyst was exposed to a flow of 5.98% CO_2/He or 5% NH_3/He (50 mL min^{-1}) for 1 h, we removed the residual gases by purging with pure He for 1 h at either 313 K for CO_2 or at 473 K for NH_3. TPD profiles were obtained by ramping up the temperature at a heating rate of 5 K min^{-1} under He (50 mL min^{-1}) to either 1073 K for the CO_2-TPD or to 1173 K for the NH_3-TPD. The CO_2- and NH_3-TPD profiles were normalized by the weight of sample. 3) For the physisorption of nitrogen (BET measurement) and the chemisorptions of carbon monoxide, we used ASAP 2010 and Autochem 2910 apparatus (Micrometrics). The nitrogen physisorption measurement was taken at 77 K. Before the measurement, all the samples were degassed and dehydrated at 573 K. In the case of the chemisorption of carbon monoxide, the catalysts were reduced at each temperature determined by TPR. The reactor was then kept at 573 K for 1 h to remove the absorbed hydrogen. The chemisorption was conducted after cooling to 323 K. For computing the CO uptake of the nickel catalysts, a value of 1.4 for the Ni/CO stoichiometry was used.[23] 4) XRD patterns of each calcined and reduced catalyst were obtained by using a Rigaku D/MAX-III X-ray diffractometer with nickel-filtered CuK_α radiation (40 kV and 40 mA). It was then measured at 2° steps in the 2-theta range of 20–80°. The average particle diameter is derived from Scherrer's equation. 5) Catalyst profiles derived from TG/DTA were analyzed by using a TG209F3 instrument (Netzsch). After all the catalysts were dehydrated and degassed at 373 K for 2 h, they were heated to 1173 K at a heating rate of 5 K min^{-1} in air. 6) The morphology and particle size of the reduced and used catalysts were analyzed by using a HD-2300 STEM instrument (Hitach). The distribution of elements was measured by using a TEM-EDAX instrument. To analyze the carbon element, a non-carbon tape TEM grid was used to map all the catalysts.

Acknowledgements

This work has been supported by the World Class University Program (R31-2008-000-10055-0) and the Advanced Biomass R&D Center (ABC) of Korea Grant funded by the Ministry of Education, Science and Technology (2011).

Keywords: carbides · heterogeneous catalysis · nickel · renewable resources · supported catalysts

[1] S. Zinoviev, F. Müller-Langer, P. Das, N. Bertero, P. Fornasiero, M. Kaltschmitt, G. Centi, S. Miertus, *ChemSusChem* **2010**, *3*, 1106 – 1133.

[2] a) F. Ma, M. A. Hanna, *Bioresour. Technol.* **1999**, *70*, 1 – 15; b) P. Bondioli, *Top. Catal.* **2004**, *27*, 77 – 82.

[3] J. M. Encinar, J. F. González, A. Rodríguez-Reinares, *Ind. Eng. Chem. Res.* **2005**, *44*, 5491 – 5499.

[4] M. Pagliaro, R. Ciriminna, H. Kimura, M. Rossi, C. Della Pina, *Angew. Chem.* **2007**, *119*, 4516 – 4522; *Angew. Chem. Int. Ed.* **2007**, *46*, 4434 – 4440.

[5] a) H. Kimura, K. Tsuto, T. Wakisaka, Y. Kazumi, Y. Inaya, *Appl. Catal. A* **1993**, *96*, 217 – 228; b) J. M. Clacens, Y. Pouilloux, J. Barrault, *Appl. Catal. A* **2002**, *227*, 181 – 190; c) S. Demirel-Gülen, M. Lucas, P. Claus, *Catal. Today* **2005**, *102 – 103*, 166 – 172; d) R. R. Soares, D. A. Simonetti, J. A. Dumesic, *Angew. Chem.* **2006**, *118*, 4086 – 4089; *Angew. Chem. Int. Ed.* **2006**, *45*, 3982 – 3985; e) S. Demirel, K. Lehnert, M. Lucas, P. Claus, *Appl. Catal. B* **2007**, *70*, 637 – 643; f) K. Klepácová, D. Mravec, A. Kaszonyi, M. Bajus, *Appl. Catal. A* **2007**, *328*, 1 – 13; g) E. P. Maris, R. J. Davis, *J. Catal.* **2007**, *249*, 328 – 337; h) M. Akiyama, S. Sato, R. Takahashi, K. Inui, M. Yokota, *Appl. Catal. A* **2009**, *371*, 60 – 66; i) B. Katryniok, S. Paul, M. Capron, F. Dumeignil, *ChemSusChem* **2009**, *2*, 719 – 730; j) D. C. Rennard, J. S. Kruger, L. D. Schmidt, *ChemSusChem* **2009**, *2*, 89 – 98; k) M. Sankar, N. Dimitratos, D. W. Knight, A. F. Carley, R. Tiruvalam, C. J. Kiely, D. Thomas, G. J. Hutchings, *ChemSusChem* **2009**, *2*, 1145 – 1151.

[6] a) M. Bowker, P. Davies, L. Al-Mazroai, *Catal. Lett.* **2009**, *128*, 253 – 255; b) I. N. Buffoni, F. Pompeo, G. F. Santori, N. N. Nichio, *Catal. Commun.* **2009**, *10*, 1656 – 1660; c) C. A. Henao, D. Simonetti, J. A. Dumesic, C. T. Maravelias, *Comp. Aid. Chem. Eng.* **2009**, *27*, 1719 – 1724; d) E. L. Kunkes, R. R. Soares, D. A. Simonetti, J. A. Dumesic, *Appl. Catal. B* **2009**, *90*, 693 – 698; e) P. D. Vaidya, A. E. Rodrigues, *Chem. Eng. Technol.* **2009**, *32*, 1463 – 1469; f) C. K. Cheng, S. Y. Foo, A. A. Adesina, *Catal. Commun.* **2010**, *12*, 292 – 298; g) V. Chiodo, S. Freni, A. Galvagno, N. Mondello, F. Frusteri, *Appl. Catal. A* **2010**, *381*, 1 – 7; h) A. Iriondo, V. L. Barrio, J. F. Cambra, P. L. Arias, M. B. Guemez, M. C. Sanchez-Sanchez, R. M. Navarro, J. L. G. Fierro, *Int. J. Hydrogen Energy* **2010**, *35*, 11622 – 11633; i) D. L. King, L. Zhang, G. Xia, A. M. Karim, D. J. Heldebrant, X. Wang, T. Peterson, Y. Wang, *Appl. Catal. B* **2010**, *99*, 206 – 213; j) F. Pompeo, G. Santori, N. N. Nichio, *Int. J. Hydrogen Energy* **2010**, *35*, 8912 – 8920; k) E. A. Sánchez, M. A. D'Angelo, R. A. Comelli, *Int. J. Hydrogen Energy* **2010**, *35*, 5902 – 5907; l) A. O. Menezes, M. T. Rodrigues, A. Zimmaro, L. E. P. Borges, M. A. Fraga, *Renewable Energy* **2011**, *36*, 595 – 599.

[7] a) B. Zhang, X. Tang, Y. Li, Y. Xu, W. Shen, *Int. J. Hydrogen Energy* **2007**, *32*, 2367 – 2373; b) X. Wang, N. Wang, M. Li, S. Li, S. Wang, X. Ma, *Int. J. Hydrogen Energy* **2010**, *35*, 10252 – 10256.

[8] H. M. Swaan, V. C. H. Kroll, G. A. Martin, C. Mirodatos, *Catal. Today* **1994**, *21*, 571 – 578.

[9] T. Montini, R. Singh, P. Das, B. Lorenzut, N. Bertero, P. Riello, A. Benedetti, G. Giambastiani, C. Bianchini, S. Zinoviev, S. Miertus, P. Fornasiero, *ChemSusChem* **2010**, *3*, 619 – 628.

[10] C. Rhodes, G. J. Hutchings, A. M. Ward, *Catal. Today* **1995**, *23*, 43 – 58.

[11] J. C. Serrano-Ruiz, J. Luettich, A. Sepúlveda-Escribano, F. Rodríguez-Reinoso, *J. Catal.* **2006**, *241*, 45 – 55.

[12] E. L. Kunkes, E. I. Gürbüz, J. A. Dumesic, *J. Catal.* **2009**, *266*, 236 – 249.

[13] G. Li, L. Hu, J. M. Hill, *Appl. Catal. A* **2006**, *301*, 16 – 24.

[14] Z. Y. Hou, O. Yokota, T. Tanaka, T. Yashima, *Catal. Lett.* **2003**, *89*, 121 – 127.

[15] a) A. Basinska, L. Kepinski, F. Domka, *Appl. Catal. A* **1999**, *183*, 143 – 153; b) Y. Li, Q. Fu, M. Flytzani-Stephanopoulos, *Appl. Catal. B* **2000**, *27*, 179 – 191; c) R. J. Gorte, S. Zhao, *Catal. Today* **2005**, *104*, 18 – 24; d) P. Panagiotopoulou, D. I. Kondarides, *Catal. Today* **2006**, *112*, 49 – 52.

[16] H. K. W. Girke, D. Arntz, T. Haas, A. Neher, US Patent 5387720, **1995**.

[17] S. M. Kim, M. E. Lee, J.-W. Choi, D. J. Suh, Y.-W. Suh, *Catal. Commun.* **2011**, *16*, 108 – 113.

[18] Y. Choi, N. D. Kim, J. Baek, W. Kim, H. J. Lee, J. Yi, *Int. J. Hydrogen Energy* **2011**, *36*, 3844 – 3852.

[19] M.-F. S. G. Reyniers, G. F. Froment, *Ind. Eng. Chem. Res.* **1995**, *34*, 773 – 785.

[20] R. R. Davda, J. W. Shabaker, G. W. Huber, R. D. Cortright, J. A. Dumesic, *Appl. Catal. B* **2005**, *56*, 171 – 186.

[21] a) E. C. Wanat, K. Venkataraman, L. D. Schmidt, *Appl. Catal. A* **2004**, *276*, 155 – 162; b) H. Liu, W. Chen, *Corros. Sci.* **2007**, *49*, 4134 – 4153; c) T. Montini, L. De Rogatis, V. Gombac, P. Fornasiero, M. Graziani, *Appl. Catal. B* **2007**, *71*, 125 – 134.

[22] a) H. Liu, S. Li, S. Zhang, L. Chen, G. Zhou, J. Wang, X. Wang, *Catal. Lett.* **2008**, *120*, 111 – 115; b) H. Liu, S. Li, S. Zhang, J. Wang, G. Zhou, L. Chen, X. Wang, *Catal. Commun.* **2008**, *9*, 51 – 54.

[23] K. Ahmed, L. S. Kershenbaum, D. Chadwick, *Ind. Eng. Chem. Res.* **1990**, *29*, 150 – 156.

Received: December 18, 2011
Published online on June 29, 2012

